Electronic Supplementary Material (ESI) for Materials Chemistry Frontiers.

Electronic Supplementary Information

Rubbing-assisted approach for highly-oriented collagen fibril arrays involving calcium phosphate precipitation

Yadong Chai [a], Mitsuhiro Okuda [b, c], Mari Miyata [d],

Zizhen Liu [a], Motohiro Tagaya [a, *]

[a] *Department of Materials Science and Technology, Nagaoka University of Technology, Kamitomioka 1603-1, Nagaoka, Niigata 940-2188, Japan*

[b] *CIC nanoGUNE consolider, Avenida Tolosa 76, E-20018, Donostita-San Sebastian, Spain*

[c] *IKERBASQUE, Basque Foundation for Science, 48011 Bilbao, Basque Country, Spain*

[d] *Department of Materials Engineering, National Institute of Technology, Nagaoka College, Nagaoka, Japan, 940-8532, Japan*

*** Author to whom correspondence should be addressed:**

Tel: +81-258-47-9345, Fax: +81-258-47-9300, E-mail: tagaya@mst.nagaokaut.ac.jp

Figure S1

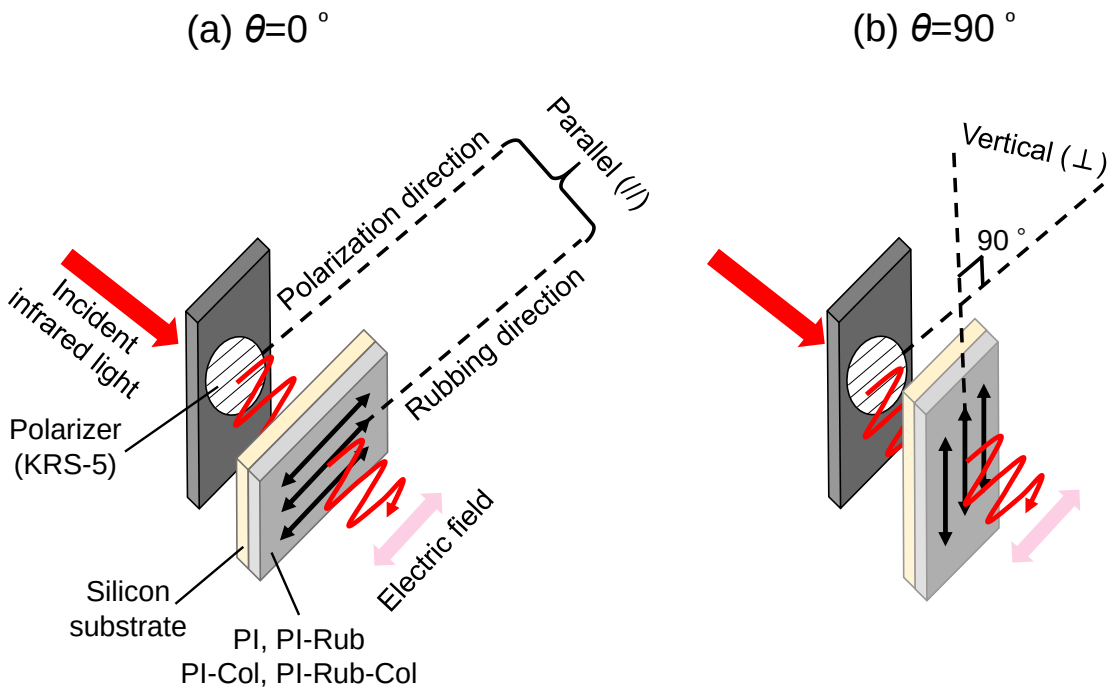

Figure S1. Illustration of the polarized FT-IR measurement systems. (a) the state of "polarization direction // rubbing direction" was named as "θ=0 °", and (b) the state of "polarization direction ⊥ rubbing direction" was named as "θ=90 °". The θ value was changed from 0 ° to 90 °.

Figure S2

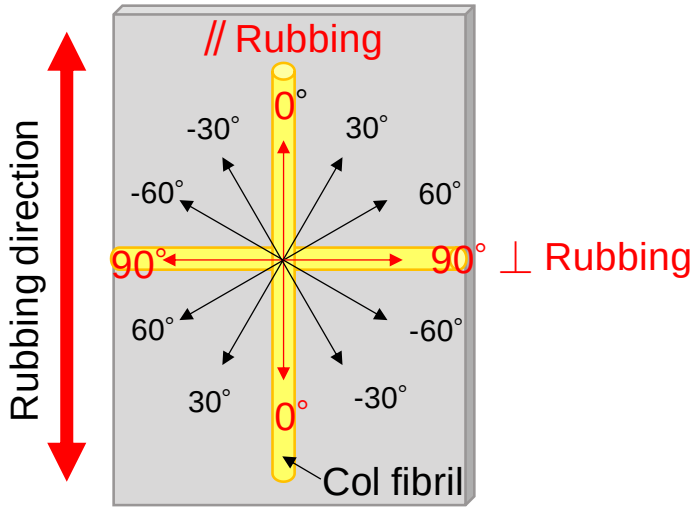

Figure S2. Calculation method of O.R. values of Col fibrils on the PI and PI-Rub.

Figure S3

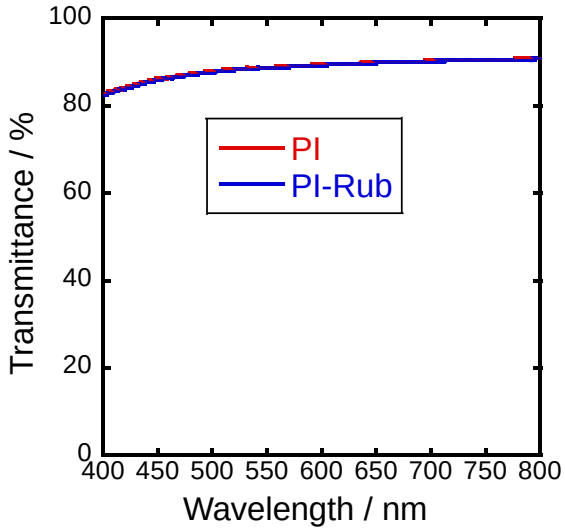

Figure S3. UV-Vis spectra of the PI and PI-Rub films where the averaged transmittance values (wavelengths in a visible light region: 400−800 nm) were 88.8 % and 88.6 %, respectively.

Figure S4

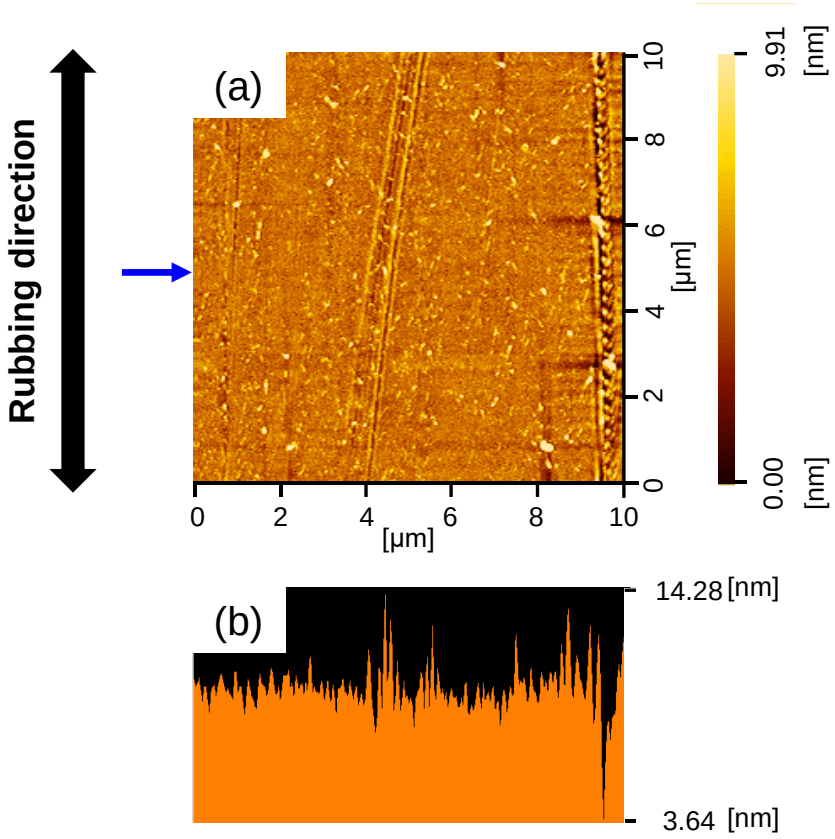

Figure S4. Representative (a) AFM topographic image of the PI-Rub film and (b) the height profile taken along the direction of blue-color arrow in (a).

Figure S5

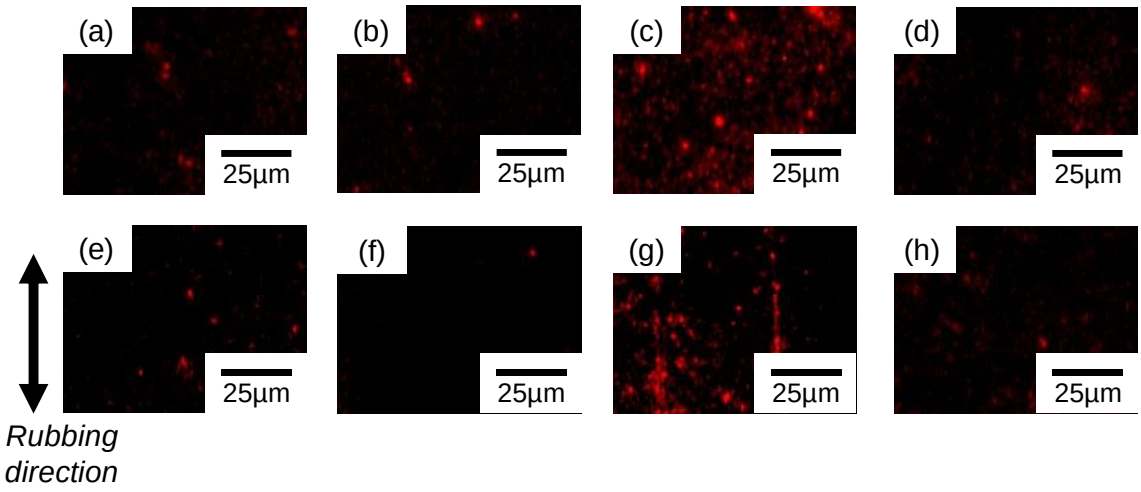

Figure S5. Fluorescence microscope images of (a) PI-CM/3, (b) PI-CM/9, (c) PI-AM/3, (d) PI-AM/9, (e) PI-Rub-CM/3, (f) PI-Rub-CM/9, (g) PI-Rub-AM/3, (h) PI-Rub-AM/9 where (a, b, e, f) carboxyl-modified and (c, d, g, h) amino-modified fluorescent poly(styrene) particles adsorbed on (a-d) PI and (e-h) PI-Rub films at the solution pH values of (a, c, e, g) 3 and (b, d, f, h) 9. In particular, (c) amino-modified fluorescent poly(styrene) particles were randomly adsorbed on PI film and (g) were adsorbed along the rubbing direction on PI-Rub film.

Figure S6

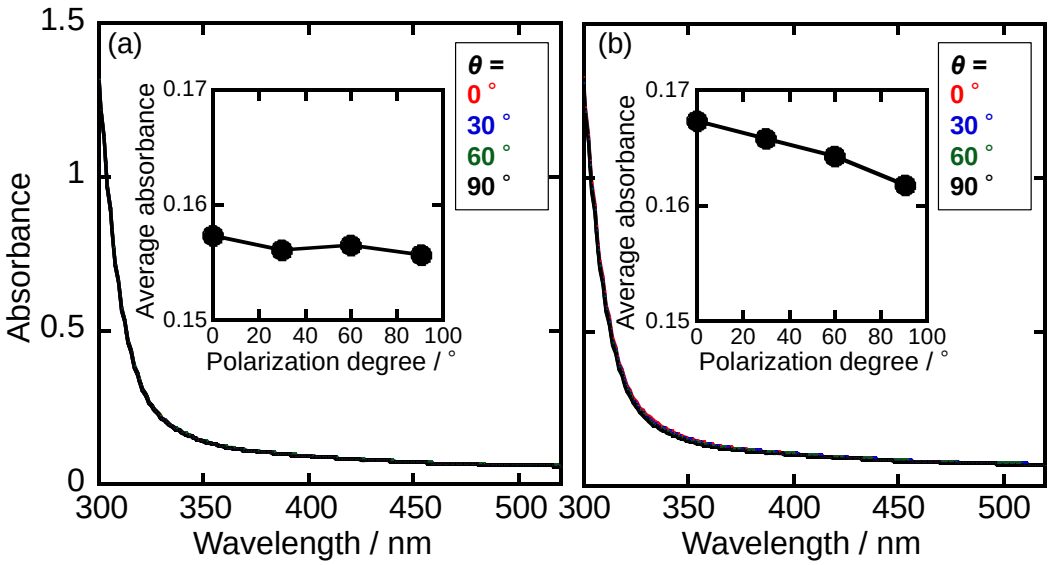

Figure S6. Polarized UV-Vis spectral changes of (a) PI-AM/3 and (b) PI-Rub-AM/3 films.

Figure S7

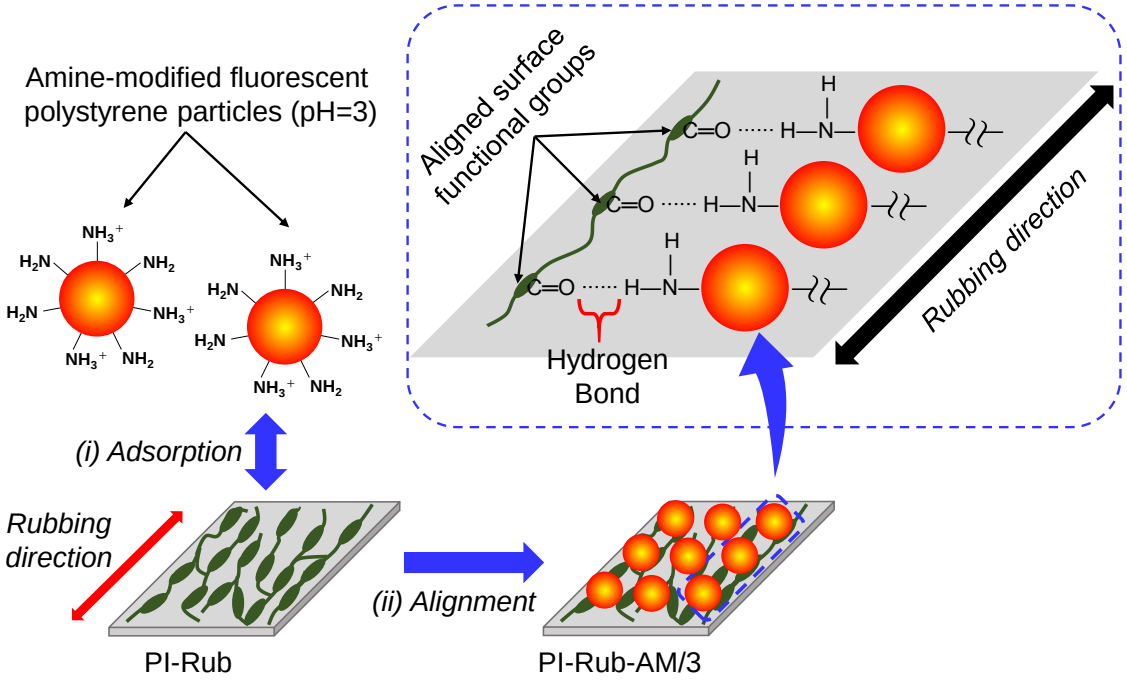

Figure S7. Illustration of the interfacial interaction mechanism between amino-modified fluorescent poly(styrene) particles and PI-Rub film.

Figure S8

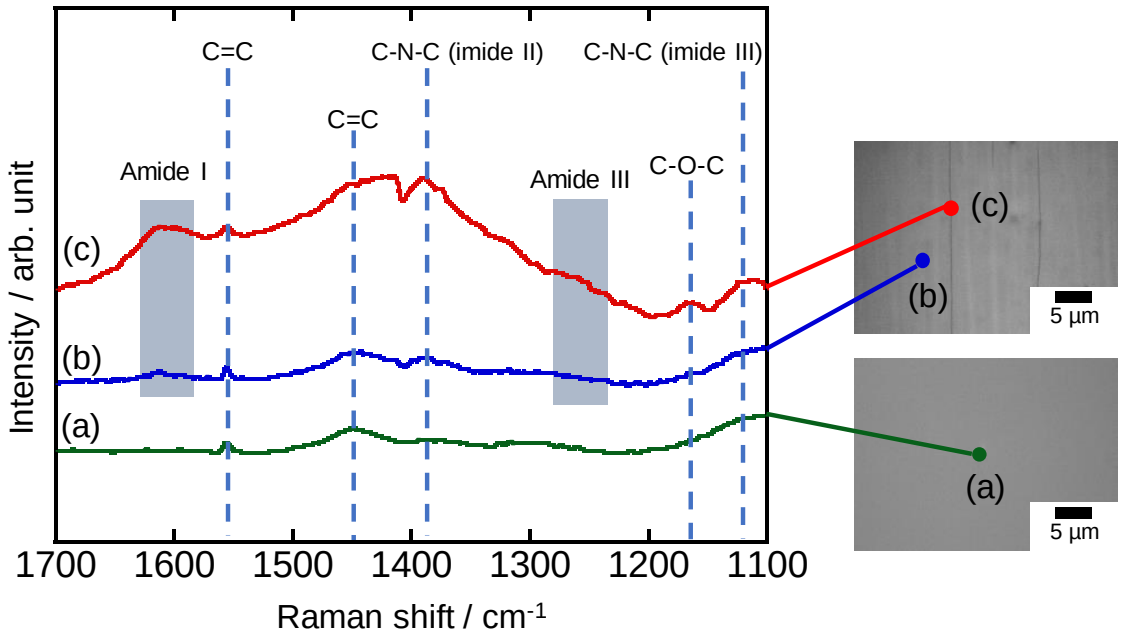

Figure S8. Raman spectra of (a) PI-Rub, and (b, c) PI-Rub-Col/**3**. Here, the Col fibrils that were (b) absence and (c) presence in PI-Rub-Col/**3** were measured.

Table S1

Table S1. Absorption band assignments of the FT-IR spectra of PI-Col/**3** and PI-Rub-Col/**3** in Figure 4 (a, b).

Wavenumber / cm^{-1}	Attribution	Bonding state
1242	C–O–C	Stretching
1377	C–N in imide	Stretching
1500	C=C in benzene ring	Stretching
1555	N–H and C–N in amide II	(N–H) In-plane bending and (C–N) Stretching
1658	C=O in amide I	Stretching
1723	C=O in imide functional group	Asymmetric stretching
1778	C=O in imide functional group	Symmetric stretching

Figure S9

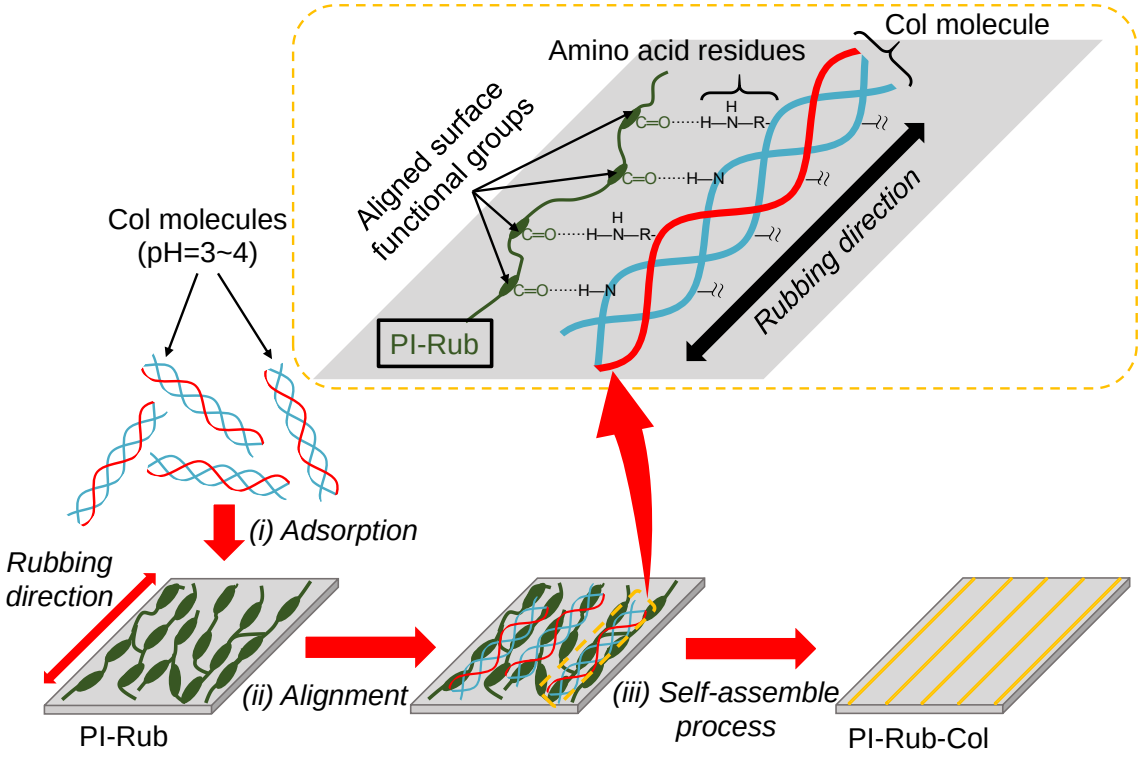

Figure S9. Illustration of the highly-oriented processes of the Col fibrils on PI-Rub film.

Figure S10

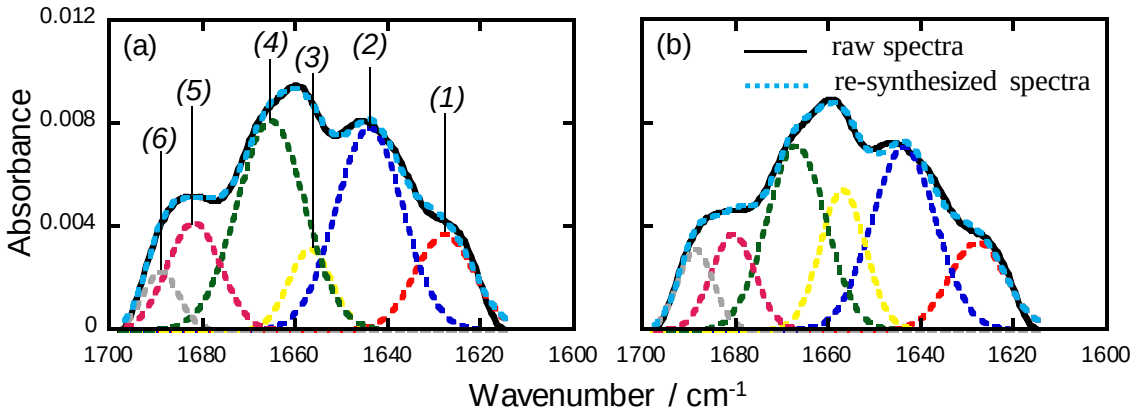

Figure S10. FT-IR spectral deconvolution results of the amide I bands of Col fibrils from (a) PI-Col/**3** and (b) PI-Rub-Col/**3**, where the secondary structural components ratios of (*1*) β-sheet were 12.5±0.3 % and 12.2±0.6 %, (*2*) random coil were 29.1±1.0 % and 27.1±1.6 %, (*3*) α-helix were 10.3±1.8 % and 18.2±1.9 %, (*4*) turn were 31.3±0.9 % and 29.5±3.8 %, (5) β-turn (1) were 10.5±1.6 % and 8.6±2.1 % and (6) β-turn (2) were 6.3±1.5 % and 4.4±2.0 %, respectively.

Figure S11

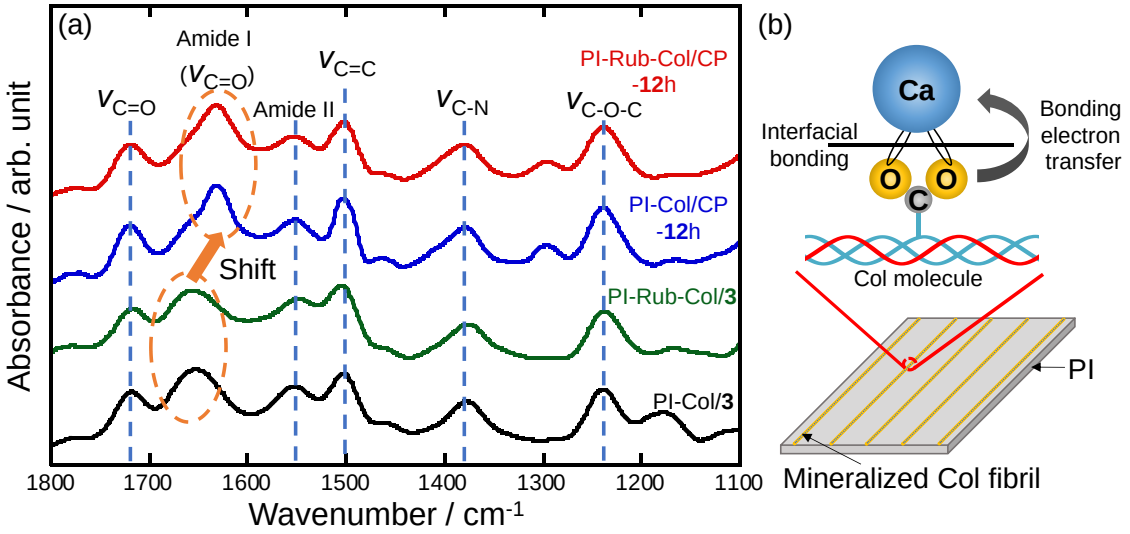

Figure S11. (a) FT-IR spectra of PI-Col/**3**, PI-Rub-Col/**3**, PI-Col/CP-**12**h and PI-Rub-Col/CP-**12**h. (b) Illustration of the possible interfacial structure between Ca^{2+} ion and Col fibril.

Figure S12

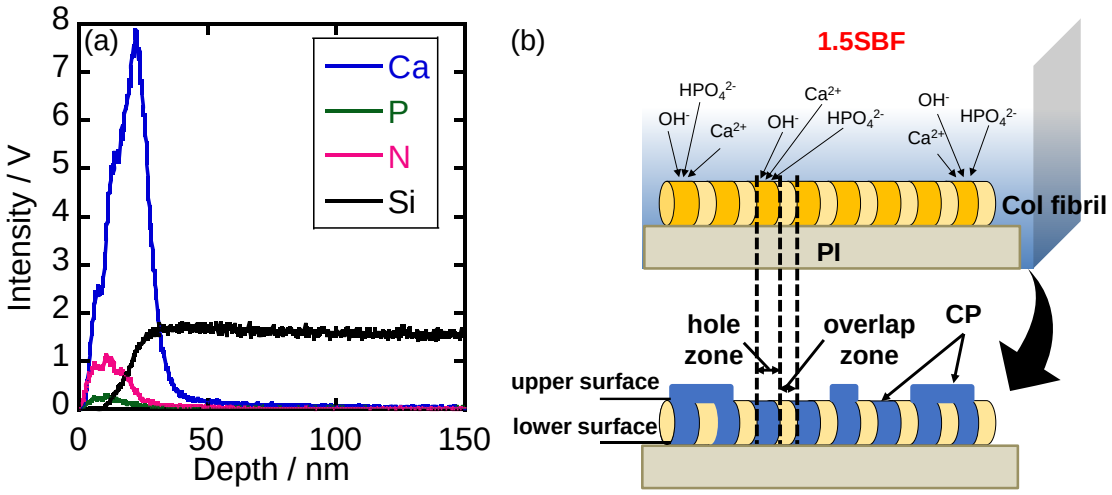

Figure S12. (a) GD-OES chemical composition profiles of PI-Rub-Col/CP-**12**h. (b) Illustration of the precipitation of CP on the hole zone of Col fibril by immersing into 1.5SBF.

Figure S13

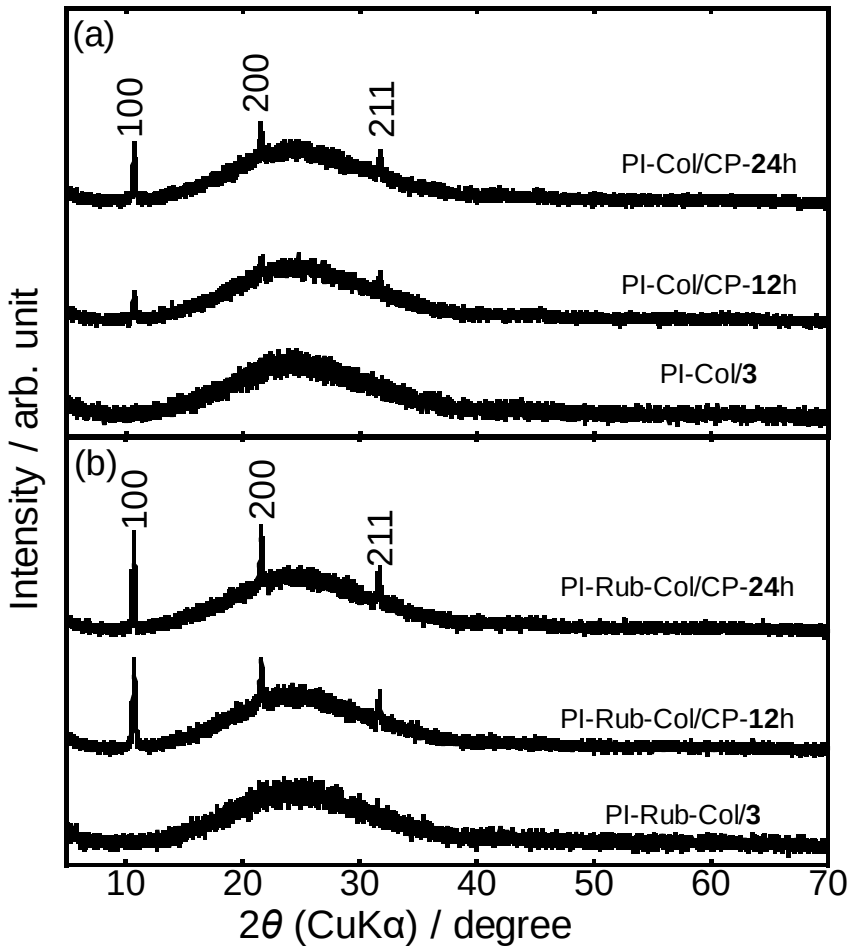

Figure S13. XRD patterns of (a) PI-Col/**3,** PI-Col/CP-**12**h, PI-Col/CP-**24**h and (b) PI-Rub-Col/**3,** PI-Rub-Col/CP-**12**h, PI-Rub-Col/CP-**24**h. The patterns of PI-Col/CP-**12**h, PI-Col/CP-**24**h, PI-Rub-Col/CP-**12**h and PI-Rub-Col/CP-**24**h were possibly attributed to a HAp single phase (JCPDS 00-009-0432, $Ca_{10}(PO_4)_6(OH)_2$).

Figure S14

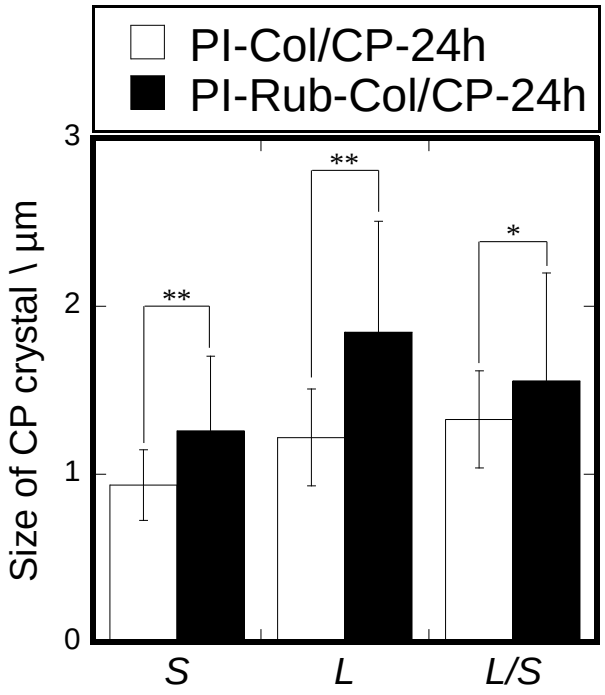

Figure S14. The short (*S*) and long(*L*) axis sizes, and the aspect ratio (*L/S*) of the CP crystals precipitated on PI-Col/CP-**24**h and PI-Rub-Col/CP-**24**h were calculated form the SEM images. Here, the student's *t*-test results were represented by $p < 0.05$ (*) and $p < 0.01$ (**).